RESIN IMPREGNATION FOR CONTINUOUS CARBON FIBRES USING ROLLERS

YUJI KONDO, KOYA HOSOKAWA, TATSUYA TANAKA & MASAHIRO SASADA
Department of Mechanical Engineering, Graduate School of Science and Engineering,
Doshisha University, Japan

ABSTRACT

In the pursuit of high-quality and high-strength continuous fibre-reinforced thermoplastic (CFRTP) filaments, enhancing fibre dispersibility is critical. This study focuses on enhancing the fibre spreading mechanism via the roller method, a process that was previously inaccessible to observation due to the use of resin-filled equipment. To overcome this limitation, an experimental apparatus was developed that enabled in situ visualization of fibres' behaviour. In the conventional roller spreading method, the cylindrical rollers had limitations in fibre spreading. An alternative approach employing inclined rollers was then tested; however, excessive inclination led to a pronounced central bias of the fibres, further hindering uniform dispersion. To address this challenge, we devised a roller with a curved shape designed to mitigate fibre bias while increasing the spreading width. Continuous fibre-reinforced filaments were produced using this innovative geometry, and the effects on fibre dispersibility and void area were evaluated at pull speeds of 1 m/min and 2 m/min. The findings of the study demonstrated that the curved roller reduced the void area and a modest enhancement in fibre dispersibility when compared to traditional cylindrical rollers. These observations suggest that the curved roller design is effective in producing superior quality CFRTP filaments and indicate a promising potential for further improvements in composite material performance.

Keywords: CFRTP, fibre spreading, roller spreading method.

1 INTRODUCTION

Carbon fibre reinforced thermoplastics (CFRTPs) have attracted attention as a promising material due to their high mechanical properties, short moulding cycle times, and recyclability. These characteristics render CFRTPs well-suited for the reduction of weight in large transportation equipment, such as automobiles, by replacing metal components and thereby reducing environmental impact [1].

One of the manufacturing methods for CFRTP is pultrusion, wherein continuous carbon fibre bundles are drawn through a resin-impregnation bath containing molten thermoplastic resin. This process impregnates the fibre bundles with resin, forming CFRTP strands that serve as intermediate materials, such as long-fibre pellets or unidirectional (UD) tapes, for various applications [2]. In the context of continuous-fibre CFRTP, it has been established that fibre spreading enhances fibre dispersion, thereby promoting impregnation and leading to enhanced mechanical strength [3]. To achieve fibre spreading, roller-based or air-jet methods are commonly employed prior to the impregnation process [4].

In this study, the focus is on a molten-impregnation method that utilizes a roller-based approach (henceforth referred to as the 'roller-spreading method') to enable simultaneous fibre spreading and resin impregnation. Specifically, a spreading roller is placed inside the molten resin bath, allowing both fibre spreading and resin impregnation to occur simultaneously. The underlying mechanism of roller spreading is as follows: when a fibre bundle, impregnated with resin, is pulled out from the bath, a tensile force is generated. At the roller, this tension induces a compressive force on the fibre bundle, with the horizontal component of this compressive force acting on each filament, causing the bundle to spread. As this method relies on compressive force rather than the removal of sizing agents, bundles

WIT Transactions on The Built Environment, Vol 216, © 2025 WIT Press
www.witpress.com, ISSN 1743-3509 (on-line)
doi:10.2495/HPSM250011

with sizing can also be effectively spread. Furthermore, simultaneous execution of spreading and impregnation simultaneously enhances process productivity.

To investigate this roller-spreading method in detail, an experimental apparatus was constructed using silicone oil in place of molten thermoplastic resin, allowing for direct visualization of the spreading process. The behaviour of the fibre bundles during the spreading process was observed and the width of the bundles after spreading was measured. While conventional roller-spreading methods typically employ cylindrical rollers, previous studies have reported certain limitations associated with this roller geometry. Therefore, this study examined various roller shapes and the results are presented in the following sections.

2 ROLLER SHAPE TO IMPROVE FIBRE SPREADING WIDTH

2.1 Purpose of the experiment

The effects of impregnation bath parameters on fibre spreading using cylindrical rollers have been investigated. The experimental results with cylindrical rollers suggest that both the compressive force and the resin film influence the spread width. Therefore, to optimize fibre spreading, the focus was placed on roller geometry and the examination of shapes that could more effectively utilize compressive force. Specifically, the study explores roller geometries capable of achieving greater fibre spreading than cylindrical rollers. To evaluate the effectiveness of these rollers, they were fabricated using a 3D printer and the influence of roller shape on spread width was analysed.

2.2 Experimental methods

2.2.1 Experimental conditions

In this experiment, PAN-based carbon fibre bundles (TR50S15L, manufactured by Mitsubishi Chemical) were used. These fibre bundles consist of 15,000 filaments and have a width ranging from 6.0 to 8.0 mm. To visualize the interior of the impregnation bath, silicone oil (manufactured by Shin-Etsu Chemical Co., Ltd.) was used as a substitute for high-temperature molten resin. The silicone oil used in this experiment had a viscosity of 100,000 mm^2/s. The utilization of silicone oil is advantageous due to its colourless transparency and its relatively stable viscosity over a wide temperature range.

2.2.2 Fibre spreading experimental apparatus

The fibre spreading mechanism of the roller method remains unclear due to the inability to observe the interior of the resin impregnation bath. To address this issue, a transparent mock experimental device with the same structure as the molten resin impregnation bath was constructed (hereafter referred to as the resin impregnation bath). The structure of the resin impregnation bath is shown in Fig. 1.

In the experimental setup, a carbon fibre bundle is drawn from the carbon fibre roving, passed through the resin impregnation bath, and then wound up by a take-up motor. A high-resolution camera (Canon EOS M10) was positioned above the resin impregnation bath to capture the spreading behaviour. Initial tension (rear tension) was applied using a torque motor, as illustrated in Fig. 2.

The rollers were fabricated from ABS resin with a surface roughness of Ra 0.05. For the take-up motor, a brushless motor (BLE2D120-A, Oriental Motor Co.) was employed. Each experiment was conducted for a total duration of 6 seconds (recording time), and for all experiments described below, the number of trials was set to $N = 5$.

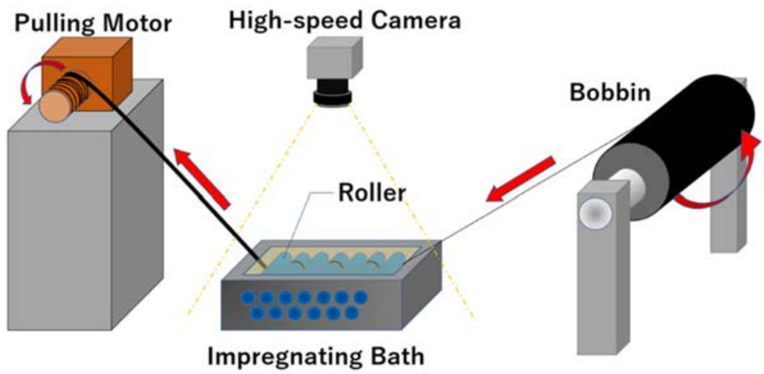

Figure 1: Model of impregnation bath.

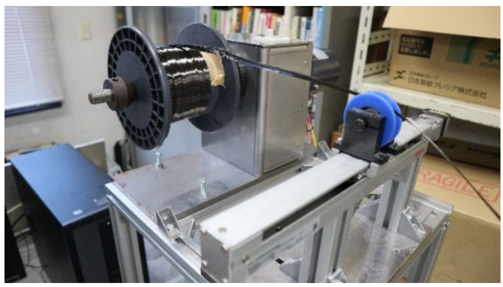

Figure 2: Equipment for back tension.

2.2.3 Methods for assessing fibre bundle spreading width

The experiment was conducted by operating the motor for a period of 6 seconds before stopping. The 6-second duration was selected to prevent alterations in fibre spreading behaviour due to the depletion of silicone oil. Subsequent to each experiment, images captured by a high-resolution camera were analysed using the software SIGMASCAN PRO to evaluate the spreading width of the fibre bundles. Due to the structural constraints of the resin impregnation bath, measurements were limited to the spreading width at every even-numbered roller.

2.2.4 3D printing of rollers

An FDM-type 3D printer (S3DP 222, S-Lab) was used to produce the rollers. The printing conditions are summarized in Table 1. ABS filament (diameter: 1.75 mm) was used as the roller material. The printing temperature was set at 260°C, and the bed temperature was maintained at 110°C. Nozzle moving speed was 2 mm/s.

Table 1: 3D print condition.

Nozzle temperature (°C)	260
Bed temperature (°C)	110
Nozzle moving speed (mm/s)	2
Layer height (mm)	1.1

After printing, the rollers were placed in a sealed container filled with acetone vapor for 40 minutes to remove layer marks from the roller surface. The surface roughness of the acetone-treated rollers was measured to be Ra 0.05.

2.2.5 Experimental conditions and roller shapes

The experimental conditions are summarized in Table 2. With regard to the roller arrangement, guide rollers were positioned before and after the test rollers, with different shapes employed to ensure that the fibre bundles remained centred on the roller (see Fig. 3).

Table 2: Experiment conditions.

Number of rollers	4
Pulling speed (m/min)	3.7
Roller diameter (mm)	13
Back tension (N)	5
Roller condition	Rotation

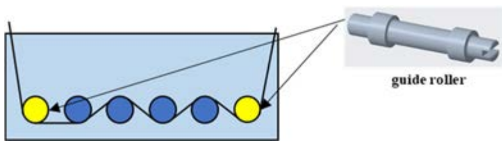

Figure 3: Rollers position.

The hypothesis was that the force acting in the spreading direction on the fibre filaments would increase by introducing an inclination to the roller, thereby enhancing fibre spreading. To investigate this hypothesis, two types of rollers were fabricated: one with a linear longitudinal profile and another with a circumferential longitudinal profile defined by an arc of circumference. The schematics and dimensions of the fabricated rollers are illustrated in Figs 4 and 5, respectively.

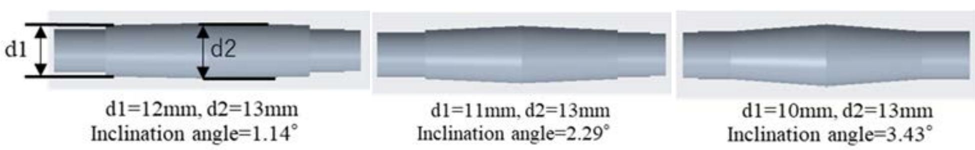

Figure 4: Roller with linear longitudinal profile.

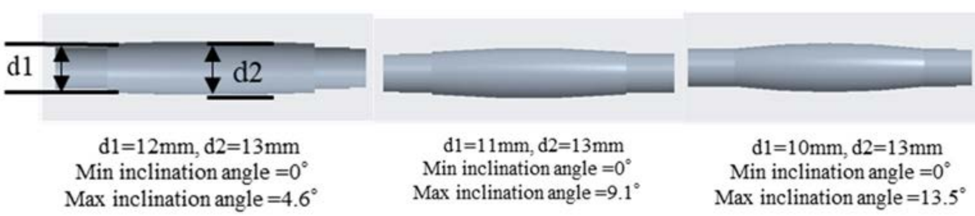

Figure 5: Roller with circumferential longitudinal profile.

The roller with a linear longitudinal profile, the purpose of which was to study the influence of the inclination angle, was designed with the following specifications: the maximum diameter of 13 mm at the central section, and three inclination angles were tested (1.14°, 2.29° and 3.43°). The roller with a circumferential profile was designed to examine the effect of the slope shape on fibre spreading. The maximum diameter at the central section of this roller was set to 13 mm, while the minimum diameters at both ends were set to 10 mm, 11 mm and 12 mm, respectively. This configuration resulted in a continuous circumferential profile connecting the centre and the ends of the roller.

2.3 Results and discussion

2.3.1 Experimental results for rollers with linear profile

The experimental measurements for fibre spreading width and tensile force obtained using rollers with a linear profile (hereafter referred to as ‘linear rollers’) are presented in Fig. 6. Fibre misalignment was observed during the experiment, as illustrated in Fig. 7. Therefore, both the spreading width measured with the misalignment and the spreading width measured without the misalignment were recorded.

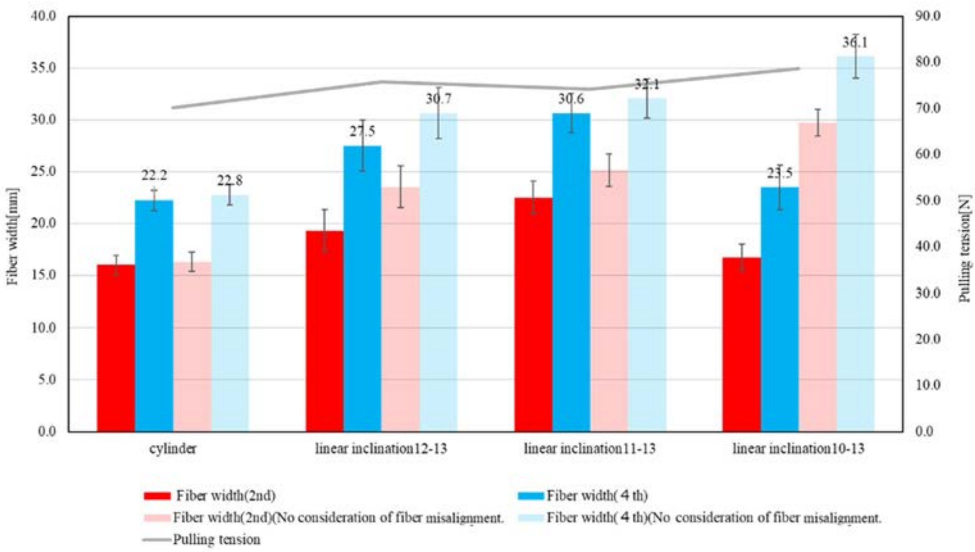

Figure 6: Experiment results using roller with linear profile (average and standard deviation of measurements).

For a slope angle of 1.14°, the average spreading width at the fourth roller was measured as 27.5 mm when considering misalignment and 30.7 mm when not considering it, with a tensile force of 75.8 N. For a slope angle of 2.29°, the average spreading width at the fourth roller was 30.6 mm considering misalignment and 32.1 mm not considering it, with a tensile force of 74.2 N. For a slope angle of 3.43°, the average spreading width at the fourth roller was 23.5 mm considering misalignment and 36.1 mm not considering it, with a tensile force of 78.7 N. In all cases, the spreading width exceeded that achieved using cylindrical rollers.

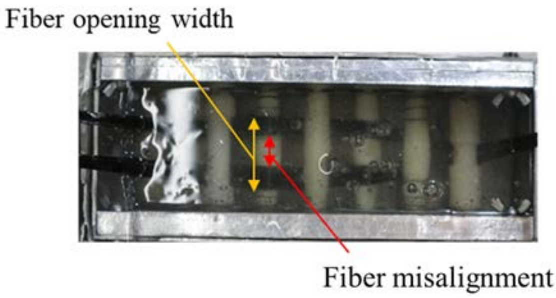

Figure 7: Experiment for rollers with linear profile.

Furthermore, the experiments confirmed that fibre misalignment became more pronounced as the slope angle increased. Fig. 7 also indicates that this misalignment occurs primarily around the central region of the roller.

2.3.2 Experimental results for rollers with circumferential longitudinal profile

Fig. 8 presents the experimental results for fibre spreading width and tensile force obtained using rollers with circumferential longitudinal profile (hereafter referred to as 'curved rollers'). As with the rollers featuring a linear profile, the spreading width was measured with and without accounting for fibre misalignment.

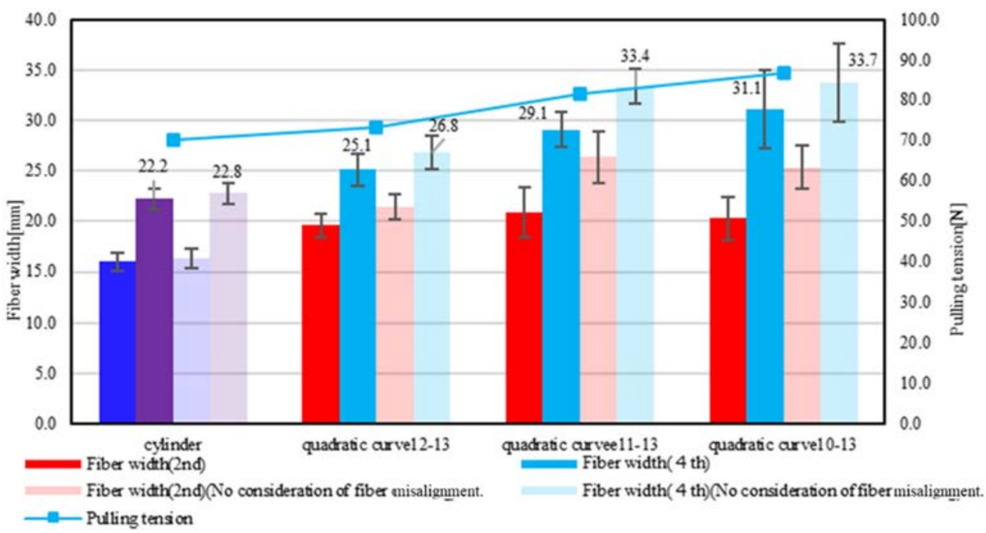

Figure 8: Experiment results using rollers with circumferential profile (average and standard deviation of measurements).

For the profile 12–13 (maximum slope angle of 4.6°, see Fig. 5), the average spreading width at the fourth roller was measured to be 25.1 mm when considering misalignment and 26.8 mm when not considering it, with a tensile force of 73.5 N. With a maximum slope angle of 9.1° (profile 11–13), the average spreading width was 29.1 mm considering misalignment and 33.4 mm not considering it, with a tensile force of 81.5 N. The profile 10–13 (maximum slope angle of 13.5°) showed an average spreading width of 31.1 mm considering misalignment and of 33.7 mm not considering it, with a tensile force of 86.8 N.

As illustrated in Fig. 9, the experimental image reveals that there was barely visible occurrence of fibre misalignment, thereby demonstrating that the fibres were distributed in an ideal manner for impregnation. Even at the maximum slope angle, no misalignment was observed, suggesting that the curved geometry effectively suppresses fibre misalignment. Furthermore, across all tested dimensions, the curved rollers achieved a greater spreading width than the cylindrical rollers.

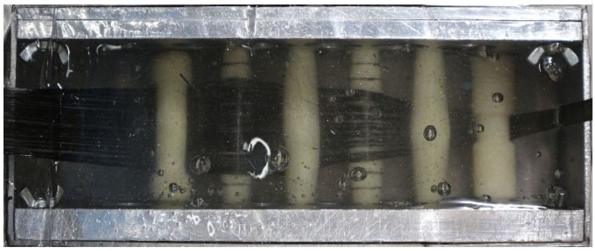

Figure 9: Experiment for rollers with circumferential profile.

3 EVALUATION USING 3K CARBON FIBRE BUNDLES

The aim of this phase of the research was to fabricate and evaluate samples using a roller with circumferential profile, which was found to enhance fibre spreading width. 3K carbon fibre bundles were used for manufacturing. By assessing the quality of the filaments produced by the actual machine, the effectiveness of the curved roller shape was validated.

3.1 Experimental materials, setup and measurements

Polyetherimide (PEI) was used as the matrix material, while PAN-based carbon fibre tow, consisting of 3,000 filaments, was used as the reinforcement material. The diameter of the carbon fibres was 7 µm.

The experimental conditions are outlined in Table 3. Five rollers were placed in the impregnation bath, with the second, third, and fourth rollers used to compare cylindrical and curved rollers.

Table 3: Experiment conditions.

Resin	PEI
Number of fibres	3K
Resin temperature (°C)	400
Number of pins	5
Speed (m/min)	1, 2

The cross-sections of the fabricated filaments were observed using imaging analysis. A compact scanning electron microscope (SEM) (TM3030+) was employed for the observations. Prior to imaging, the samples were embedded in resin and polished to obtain a smooth cross-sectional surface.

To analyse the void area, the image processing software Sigma Scan Pro 5 was used to measure the number of pixels corresponding to void regions, from which the void area was calculated. A smaller void area indicates higher impregnation quality.

To evaluate fibre dispersion, the centroid distance of carbon fibres (Voronoi region) was utilized, as shown in Fig. 10. A Voronoi diagram partitions a plane based on the proximity of each point to its nearest neighbouring point. The homogeneity coefficient H was calculated using the average area and standard deviation of the Voronoi regions and is expressed as follows [5]:

$$H = \frac{\text{Standard deviation}}{\text{Average area}} \tag{1}$$

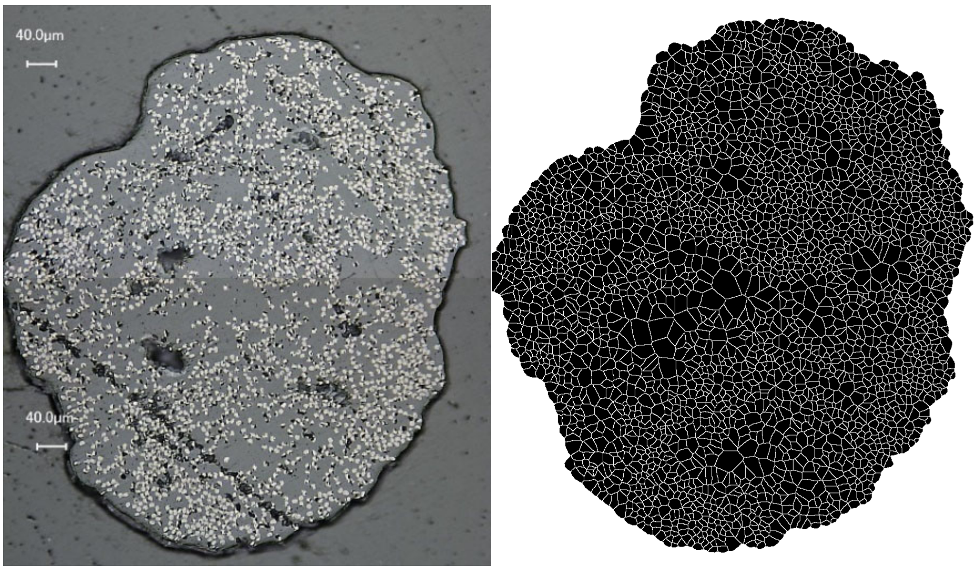

(a) (b)

Figure 10: SEM observations. (a) Cross-sectional image; and (b) Voronoi diagram.

A smaller homogeneity coefficient *H* indicates better fibre dispersion. The number of measured samples was six**.**

3.2 Experimental results

3.2.1 Measurement of void area

The results of the void area measurements obtained from the cross-sectional observations of the filaments are presented in Figs 11 and 12. Fig. 11 compares the void areas of filaments produced using cylindrical and curved rollers at a take-up speed of 1 m/min, while Fig. 12 presents the comparison at a take-up speed of 2 m/min.

At a take-up speed of 1 m/min, the average void area of the filaments was 0.000132 mm^2 for the cylindrical roller and 0.000071 mm^2 for the curved roller. Similarly, at 2 m/min, the average void area was 0.000244 mm^2 for the cylindrical roller and 0.000131 mm^2 for the curved roller.

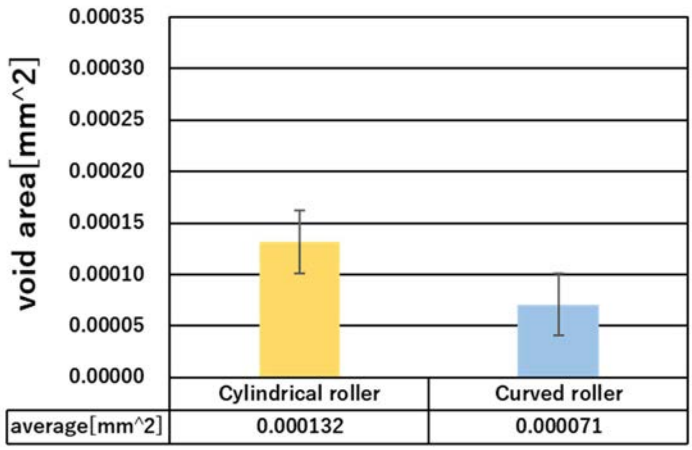

Figure 11: Void area at 1 m/min (average and standard deviation of six measurements).

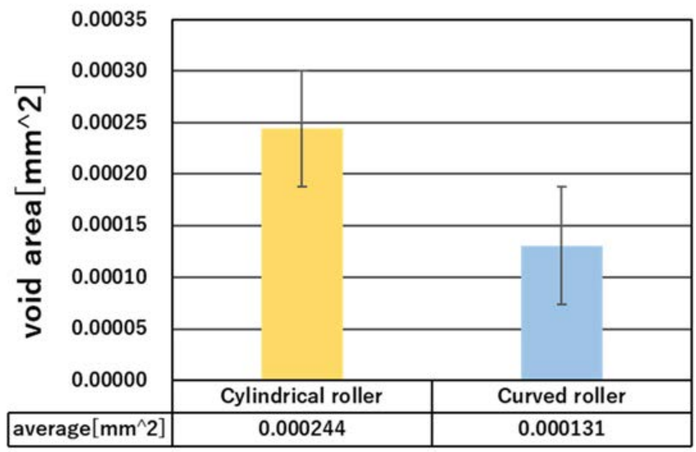

Figure 12: Void area at 2 m/min (average and standard deviation of six measurements).

An increasing void area was observed as the take-up speed increased. Furthermore, for both take-up speeds, the utilization of the curved roller resulted in a reduction in void area. Notably, even at a take-up speed of 2 m/min, the void area of filaments produced using the curved roller was reduced to a level comparable to that of filaments produced at 1 m/min using the cylindrical roller.

3.2.2 Fibre dispersibility

The homogeneity coefficients of fibre dispersibility in the filament cross-sections at take-up speeds of 1 m/min and 2 m/min are presented in Figs 13 and 14, respectively.

At a take-up speed of 1 m/min, the homogeneity coefficient was 0.83 for the cylindrical roller and 0.75 for the curved roller. A similar trend was observed at 2 m/min, the homogeneity coefficient was 0.75 for the cylindrical roller and 0.69 for the curved roller.

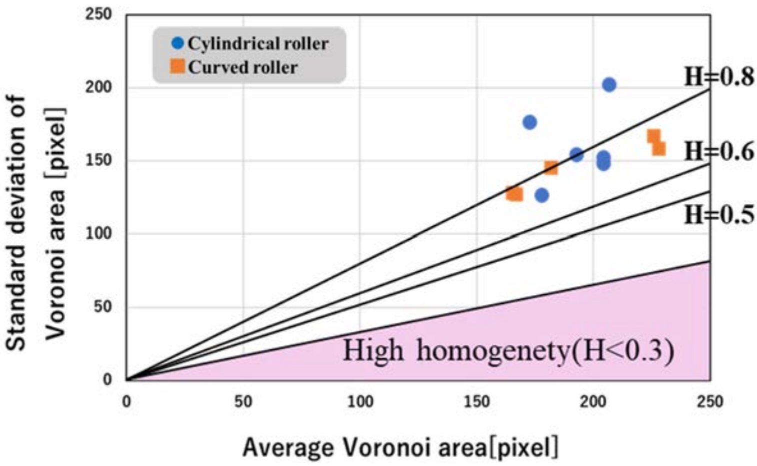

Figure 13: Results of fibre dispersibility homogeneity: take over speed 1 m/min.

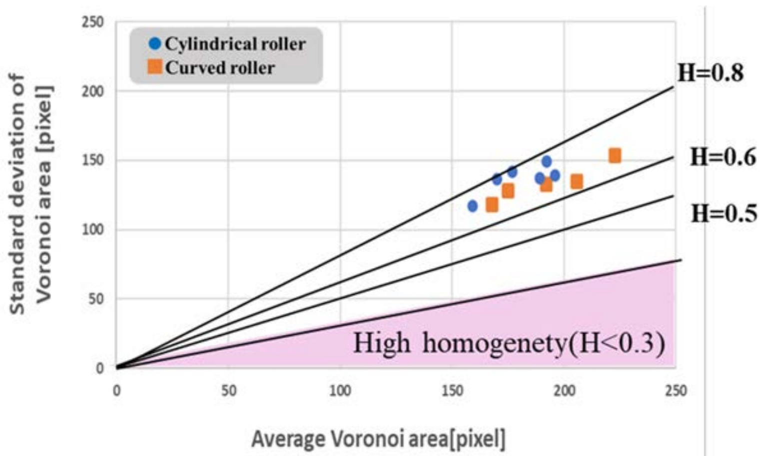

Figure 14: Results of fibre dispersibility homogeneity: take over speed 2 m/min.

Despite the use of the curved roller resulted in a reduction in the homogeneity coefficient, no substantial enhancement in fibre dispersion was observed.

4 CONCLUSIONS

The aim of this study was to improve fibre dispersibility in the production of high-quality, high-strength CFRTP filaments. In contrast to conventional resin-impregnation methods, experiments were conducted using an apparatus that allowed in situ visualization of fibre behaviour.

Initial experiments with conventional cylindrical rollers confirmed their limitations in fibre spreading, while trials with linear and circumferential longitudinal profile rollers revealed that excessive inclination resulted in a pronounced central bias of fibres. In response, a novel roller with a curved slope was devised with the aim of mitigating fibre bias and expanding the spreading width. Testing at pull speeds of 1 m/min and 2 m/min demonstrated that the curved roller significantly reduced the void area and provided a modest improvement in fibre dispersibility compared to traditional cylindrical rollers.

The findings indicate that the curved roller design offers a promising approach to enhancing CFRTP filament quality.

REFERENCES

[1] Terada, K., Carbon fibre reinforced thermoplastics (CFRTP). *Journal of the Japan Society for Precision Engineering*, **81**(6), 2015.

[2] Wakazono, T., Impregnation equipment for thermoplastic plastics. *Kobe Steel Industry Reports*, **67**(2), 2018.

[3] Tanaka, T., Fibre lengthening and dispersion technology in fibre-dispersed thermoplastic composite materials. *Journal of the Japan Society of Colour Material*, **86**(6), pp. 231–236, 2013.

[4] Kawabe, K. & Matsuo, T., Fibre bundle spreading techniques and applications to composite materials. *Journal of the Japan Society for Composite Materials*, 51(2), 2018.

[5] Hopmann, C., Wilms, E., Beste, C., Schneider, D., Fischer, K. & Stender, S., Investigation of the influence of melt-impregnation parameters on the morphology of thermoplastic UD-tapes and a method for quantifying the same. *Journal of Thermoplastic Composite Materials*, **34**(9), pp. 1299–1312, 2019.